Neutron spectrometry and dosimetry in 100 and 300 MeV quasi-mono-energetic neutron field at RCNP, Osaka University, Japan

Vladimir Mares[1,a], Sebastian Trinkl[1,2], Yosuke Iwamoto[3], Akihiko Masuda[4], Tetsuro Matsumoto[4], Masayuki Hagiwara[5], Daiki Satoh[3], Hiroshi Yashima[6], Tatsushi Shima[7], and Takashi Nakamura[8]

[1]Helmholtz Zentrum München (HMGU), 85764 Neuherberg, Germany
[2]Technische Universität München, Physik-Department, 85748 Garching, Germany
[3]Japan Atomic Energy Agency (JAEA), Tokai, Japan
[4]National Metrology Institute of Japan, National Institute of Advanced Industrial Science and Technology (NMIJ/AIST), Tsukuba, Japan
[5]High Energy Accelerator Research Organization (KEK), Tsukuba, Japan
[6]Research Reactor Institute, Kyoto University, 2-1010 Asashiro-nishi, Kumatori, Sennan, Osaka 590-0494, Japan
[7]Research Center for Nuclear Physics (RCNP), Osaka University, Mihogaoka, Ibaraki, Japan
[8]Tohoku University, Sendai, 980-0872, Japan

Abstract. This paper describes the results of neutron spectrometry and dosimetry measurements using an Extended Range Bonner Sphere Spectrometer (ERBSS) with ^{3}He proportional counter performed in quasi-mono-energetic neutron fields at the ring cyclotron facility of the Research Center for Nuclear Physics (RCNP), Osaka University, Japan. Using 100 MeV and 296 MeV proton beams, neutron fields with nominal peak energies of 96 MeV and 293 MeV were generated via ^{7}Li(p,n)^{7}Be reactions. Neutrons produced at 0° and 25° emission angles were extracted into the 100 m long time-of-flight (TOF) tunnel, and the energy spectra were measured at a distance of 35 m from the target. To deduce the corresponding neutron spectra from thermal to the nominal maximum energy, the ERBSS data were unfolded using the MSANDB unfolding code. At high energies, the neutron spectra were also measured by means of the TOF method using NE213 organic liquid scintillators. The results are discussed in terms of ambient dose equivalent, $H^*(10)$, and compared with the readings of other instruments operated during the experiment.

1 Introduction

The high-energy neutrons, which are e.g. present at flight altitudes or behind the shielding of particle accelerators or proton and ion therapy treatment facilities, need particular attention because, for example, at typical flight altitudes or outside the shielding of particle accelerators about half of the neutron ambient dose equivalent, $H^*(10)$, originates from neutrons with energies above 20 MeV [1]. Therefore, it is necessary to determine neutron dose rates associated to high-energy neutron fields as precisely as possible.

In order to monitor neutrons in high-energy fields above 20 MeV, in particular concerning dosimetry in radiotherapy, onboard aircraft and spacecraft, and radiation protection monitoring of workplaces outside high-energy accelerators, proper calibration of neutron detectors is needed. It is necessary to calibrate instruments in reference fields at energies from 20 MeV up to several hundreds of MeV - preferably in mono-energetic neutron fields - with known spectral fluence rate distribution. One of the most unique facilities worldwide which provides quasi-mono-energetic neutron fields with energies up to 400 MeV using the ^{7}Li(p,n)^{7}Be reaction is the cyclotron facility at the Research Center for Nuclear Physics (RCNP), Osaka University, Japan [2].

2 Materials and methods

2.1 RCNP facility and experimental setup

At the RCNP in Osaka the protons are pre-accelerated up to 65 MeV in an AVF cyclotron and then can be boosted up to energies of 400 MeV in the ring cyclotron. For the measurements presented in this work, proton beams with nominal energies of 100 MeV and 296 MeV were generated and focused on a 10 mm thick natLi (7.6% ^{6}Li and ^{7}Li 92.4%) target placed in a vacuum chamber (see Fig. 1). Protons passing through the target were swept out by the swinger magnet to the beam dump equipped

[a] Corresponding author: mares@helmholtz-muenchen.de

© The Authors, published by EDP Sciences. This is an open access article distributed under the terms of the Creative Commons Attribution License 4.0 (http://creativecommons.org/licenses/by/4.0/).

with a Faraday cup current monitor. The neutrons were extracted at two different emission angles, 0° and 25°, to the experimental tunnel through an iron collimator with 10x12 cm^2 aperture size embedded in a concrete wall of 1.5 m thickness at distance of 4.5 m from target.

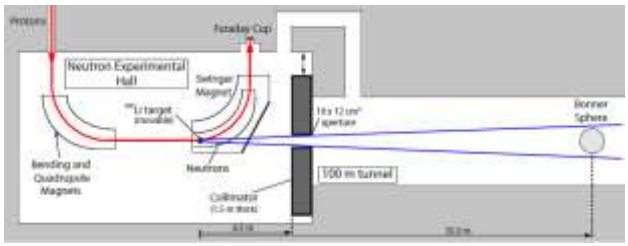

Figure 1. Sketch of the neutron experiment facility and experimental setup at the RCNP [3].

The length of the experimental tunnel is about 100 m, which enables precise measurements of neutron energy distribution above 3 MeV by the time-of-flight (TOF) method. The resulting neutron beam homogenously covered a minimum solid angle of 2.18×10^{-4} sr assuming a rotationally symmetric beam with radius 5.0 cm at the end of the collimator. At the position of the ERBSS measurement, i.e. 35 m from the target, the radius of the neutron beam was about 29 cm, which was broad enough to fully illuminate the largest sphere with its radius of 19.05 cm.

The quasi-mono-energetic neutron spectra consisted of peak neutrons and continuum component (tail), which comes from breakup reactions. The number of neutrons in peak per solid angle per electric charge was 0.87×10^{10} and 1.00×10^{10} sr^{-1} μC^{-1} for protons of 100 MeV and 296 MeV, respectively [2].

2.2 Extended range Bonner sphere spectrometer

The HMGU ERBSS system is composed of a 3.3 cm diameter spherical ^{3}He (partial pressure of 172 kPa) proportional counter type SP9 (Centronic Ltd.) and 15 polyethylene (PE) spheres of different diameters ranging from 2.5" (6.35 cm) to 15" (38.10 cm). Additionally, two 9" (22.86 cm) PE spheres are designed with lead shells of 0.5" (1.27 cm) and 1" (2.54 cm) to extend the detection range to neutrons above 10 MeV [4]. A bare ^{3}He proportional counter without any surrounding material is also used as the 18th measuring channel. This system enables accurate measurements of neutron fluence spectra, Φ(E), and ambient dose equivalent, $H^*(10)$, values, since the fluence response functions (HEMA99) of all spheres with ^{3}He proportional counter in their center were calculated by means of Monte Carlo (MC) simulations [5, 6] and experimentally validated at 13 neutron energies between thermal and 14.8 MeV [7, 8] as well as with quasi-mono-energetic neutron fields with peak energies at 244 MeV and 387 MeV [9].

3 Results and discussion

3.1 Time-of-flight spectrometry

The high-energy neutrons produced in Li target were also measured by means of the time-of-flight (TOF) method using 3 scintillator detectors [2]. The energy resolution obtained with TOF method was 1 MeV in energy region above detection threshold of 3 MeV (see Fig. 2). To allow comparison with the ERBSS spectra in Figures 3-6, the TOF spectra were rebinned to 10 log-equidistant bins per decade, which is the typical binning structure used in unfolding.

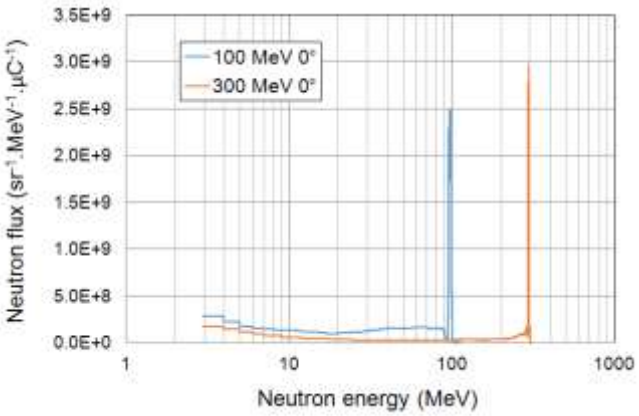

Figure 2. Neutron energy spectra at 0° for 100 MeV and 296 MeV Li(p,xn) reactions and 1 cm thick Li target using time-of-flight method.

3.2 Bonner sphere spectrometry

Using the 18 measured count rates and the HEMA99 response function, the spectral neutron fluence distribution was unfolded with the MSANDB unfolding code [10]. The resulting neutron spectra in the lethargy representation generated by protons with energy of 100 MeV and 296 MeV and emission angle of 0° are shown in Figures 3 and 4.

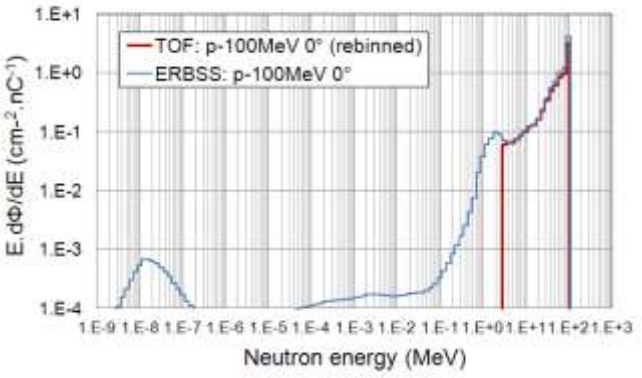

Figure 3. Neutron energy spectra at a distance of 35 m from the Li target bombarded by 100 MeV protons measured with ERBSS (thin blue line) and the TOF (thick red line) method (rebinned), at 0°.

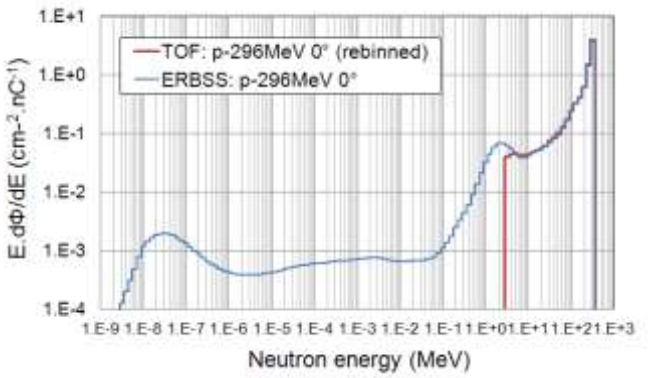

Figure 4. The same as in Fig. 3 but for 296 MeV protons.

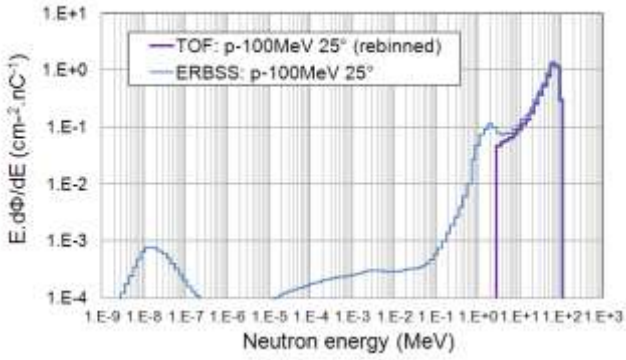

Figure 5. Neutron energy spectra at a distance of 35 m from the Li target bombarded by 100 MeV protons measured with ERBSS (thin blue line) and the TOF (thick violet line) method (rebinned), at 25°.

The neutron spectra are normalized to the proton beam current measured by a Faraday Cup (FC) inside a beam dump (see Fig. 1). The neutron spectral distributions at 0° exhibit five regions with different fluence intensity: a) a Maxwell-Boltzmann peak, b) flat epithermal region, c) an evaporation peak, d) a breakup and spallation continuum, and e) a peak region. The two most important high-energy areas of these quasi-mono-energetic neutron spectra are the continuum and peak region. As can be seen in Figures 5 and 6 the neutron spectra at 25° do not include the peak region because these neutrons produced in target – flying along the proton beam trajectory and turned 25 degree – cannot enter the TOF tunnel through aperture in 150 cm thick iron collimator embedded in a 150 cm thick concrete wall (see Fig. 1).

Both the ERBSS and the TOF neutron spectra were folded with the same fluence-to-dose $h^*(10)$ conversion coefficients to estimate the neutron ambient dose equivalent, $H^*(10)$. The conversion coefficients from ICRP 74 [11] extended to high energies with data from Pelliccioni [12] were used. These data were interpolated in the energy range between 1 meV and 10 GeV with 130 logarithmically equidistant energy bins, i.e. 10 bins per decade, for ERBSS spectra, and with 1 MeV broad bins between 3 MeV and neutron peak energy for TOF spectra (see Fig. 7).

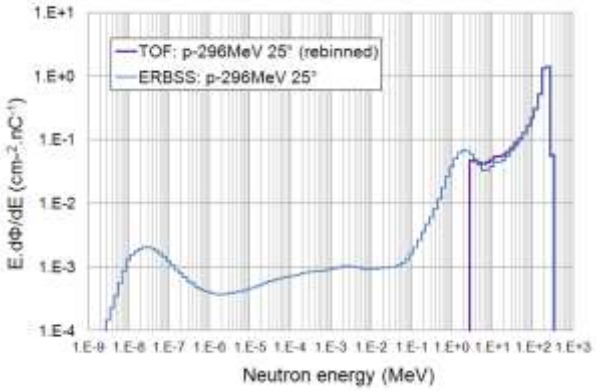

Figure 6. The same as in Fig. 5 but for 296 MeV protons.

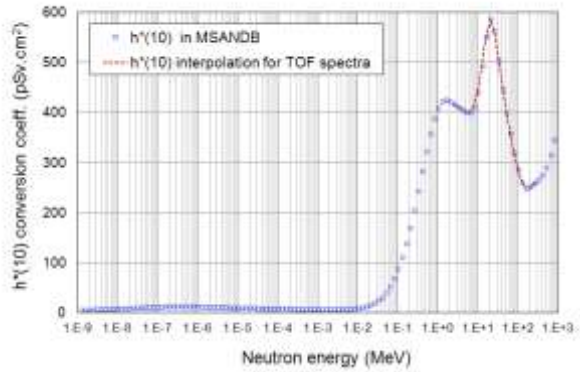

Figure 7. Neutron fluence-to-dose conversion coefficients, $h^*(10)$, as used in MSANDB unfolding code, and interpolated values for TOF spectra above 3 MeV.

In Table 1, the ERBSS $H^*(10)$ values are compared to those deduced from the TOF spectra, at 0° and 25°. Note that TOF doses were calculated in energy region above detection threshold (3 MeV). This is the reason why TOF doses are about 10 – 30 % lower than ERBSS doses.

Table 1. Neutron ambient dose equivalent, $H^*(10)$, in Sv/C, at the distance of 35 m from the target. (*contribution integrated for neutrons above 3 MeV.)

Proton energy [MeV]	Emission angle	ERBSS	TOF*
100	0°	0.79 ± 0.12	0.62 ± 0.11
100	25°	0.62 ± 0.09	0.50 ± 0.09
296	0°	0.54 ± 0.08	0.51 ± 0.09
296	25°	0.36 ± 0.05	0.33 ± 0.06

In addition, Table 2 documents the ambient dose equivalent fractions measured at 0° and 25° using ERBSS system. The neutrons measured from thermal to peak energy of 96 MeV and 293 MeV, respectively, contribute in different way to the total $H^*(10)$ in according to their energy distribution and fluence-to-dose $h^*(10)$ conversion coefficients (see Fig. 7). In Table 2 the whole energy region is divided in 4 intervals: thermal and epi-thermal ($0.01\text{eV} \leq E < 0.1$ MeV); evaporation ($0.1 \leq E < 5$ MeV); continuum ($5 \leq E <$ 96 or 293 MeV); and peak region (96 or 293 MeV). While for 296 MeV protons the continuum neutrons contribute to total H*(10) to the same degree as peak neutrons, for 100 MeV protons the continuum neutrons contribute about 60 % more than peak neutrons. The contribution of thermal and epithermal neutrons to the total $H^*(10)$ was negligible and so is not shown in Table 2.

The contribution of peak neutrons to total $H^*(10)$ was about 40 % at 0°, and almost zero at 25° for both 100 MeV and 296 MeV protons. This makes possible to obtain the response of neutron detectors to mono-energetic neutrons using the subtraction method suggested by Nolte et al. [13], applying normalization factors that equalize the $H^*(10)$ contribution below peak energy at 0° and 25°. Equalizing the $H^*(10)$ contributions in evaporation and continuum parts for 25° to that for 0°, the normalization factors of 0.861 and 0.890 for 100 MeV and 296 MeV protons, respectively, could be deduced. In this way the subtraction method can be used to simulate the calibration of neutron detectors in mono-energetic neutron fields.

Table 2. Partial contributions to the total neutron ambient dose equivalent, $H^*(10)$, in Sv/C, at the distance of 35 m from the target. The whole energy region from thermal to peak energy is divided in 4 intervals: thermal and epi-thermal ($0.01\text{eV} \leq E < 0.1$ MeV), not shown because negligible; evaporation ($0.1 \leq E < 5$ MeV); continuum ($5 \leq E <$96 or 293 MeV); and peak region (96 or 293 MeV).

Proton energy - angle	Evaporation peak	Continuum	Peak
100 MeV - 0°	0.07	0.45	0.27
100 MeV - 25°	0.07	0.52	0.02
296 MeV - 0°	0.05	0.27	0.23
296 MeV - 25°	0.05	0.30	0.00

3.3 $H^*(10)$ measurements with active detectors

In addition, neutron ambient dose equivalents, $H^*(10)$, were measured by different commercial active dosimetry systems and in-house neutron electronic dosimeter. Table 3 summarizes $H^*(10)$ values measured with ERBSS, TOF method, and active neutron dosimeters.

3.3.1 NM2B-458 and NM2B-495Pb

The Andersson‐Braun rem-counters, a conventional NM2-458 and an extended-range NM2B-495Pb model (NE Technology Ltd.), are cylindrical BF3 − boron trifluoride proportional counters surrounded by an inner polyethylene moderator, a boron-doped synthetic rubber absorber, and an outer polyethylene moderator. In the case of the NM2B-495Pb model, a 1 cm thick lead shell is added above the boron rubber to extend the detection range to higher energy neutrons. The fluence response functions from thermal to 10 GeV neutrons were calculated by means of different Monte Carlo codes [14]. All calibrations were performed in HMGU using 185 GBq ^{241}Am-Be neutron source [15]. For this experiment, pulse height spectra were registered and the number of counts in the region of interest (ROI) was then converted to $H^*(10)$ values through the calibration coefficients.

3.3.2 SNS-LINUS

This detector is an improved wide energy range detector of ambient dose equivalent. It is a combination of the NGREM spherical detector [16] with the addition of lead. The detector consists of a SP9 ^{3}He proportional counter (partial pressure of 230 kPa) covered by lead alloy, an inner polyethylene layer, a layer of 5% boron doped polyethylene surrounded by an outer polyethylene layer to bring the sphere diameter up to 240 mm. The pulse height spectra were registered and the number of counts in the ROI was then converted to $H^*(10)$ values through the calibration coefficients gained by calibration in HMGU using 185 GBq ^{241}Am-Be neutron source [14].

3.3.3 Electronic neutron dosimeter ELDO

The ELDO, neutron electronic dosimeter developed at HMGU [17], is a small (size: 115 x 60 x 16 mm^3; weight: 160 g) personal dosimeter with a dose measurement range between 1 μSv and 10 Sv. It consists of 4 Si PIN-diodes with LiF or PE converters encapsulated in Pb or Cd. Each sensor is sensitive to a certain neutron energy range and has its own calibration factor. All measured doses are summed up to provide the personal dose-equivalent, $H_p(10)$, value which is shown on LCD display. Calibration of the neutron electronic dosemeter was done at PTB (Germany) for neutron energies between 138 keV and 14.8 MeV using different target reactions [18].

4 Conclusions

The agreement between ERBSS and TOF neutron spectra above 5 MeV is very consistent. The evaporation peak around 2 MeV was only identified in ERBSS

Table 3. Neutron ambient dose equivalent, $H^*(10)$, in Sv/C, measured with active neutron dose monitors at the distance of 35 m from the target and 0° compared to ERBSS and TOF results. (*contribution integrated for neutrons above 3 MeV.) Note: ELDO is calibrated in terms of personal dose-equivalent, $H_p(10)$.

Proton energy [MeV]	ERBSS	TOF*	NM2-458	NM2B-495Pb	SNS-LINUS	ELDO
100	0.79	0.62	0.18	0.61	0.31	0.62
296	0.54	0.51	N/A	0.69	0.29	0.58

measurements because of 3 MeV detection threshold of TOF method. Comparison in terms of ambient dose equivalent, $H^*(10)$ between ERBSS and TOF values for both proton energies and emission angles shows very good agreement.

When comparing $H^*(10)$ values measured with ERBSS system and other active detectors, it was noticed that extended range detector NM2B-495Pb provides accurate (within 30%) measurement while the conventional rem-counter (NM2-458) underestimated the $H^*(10)$ by up to factor of about 4. Interestingly, the performance of SNS-LINUS range extended rem-counter was less satisfactory, it underestimated the $H^*(10)$ values up to a factor of about 2, when using a ^{241}Am-Be calibration (i.e., mean energy 4.4 MeV). This calibration may be considered responsible for the poor performance of this counter. In the case of conventional rem counters (like NM2-458), their energy response above 20 MeV, as well the detector design may be responsible for large underestimation of $H^*(10)$ in high-energy neutron fields.

The electronic neutron dosimeter ELDO was found to have good performance within 27% comparing to ERBSS values. It should also be noticed that since ELDO is calibrated in terms of $H_p(10)$, all irradiations in RCNP were done with detectors positioned over a PMMA phantom (30x30x30 cm^3). Nonetheless, comparing $H_p(10)$ and $H^*(10)$ conversion coefficients in the neutron energy range encountered in RCNP, these values can be considered equivalent with a small error less than 5 % [19] that falls within measurement uncertainties.

The authors would like to thank the staff of the RCNP, Osaka University, Japan for providing technical support, and all measurement campaign participants for their helpful cooperation and kind support during the experiment.

References

1. B. Wiegel et al., Radiat. Meas. **44**, 660-672 (2009)
2. Y. Iwamoto, M. Hagiwara, D. Satoh, S. Araki, H. Yashima et al., Nucl. Instr. and Meth. A **804**, 50–58 (2015)
3. C.D. Pioch, PhD Thesis, TU Munich (2012)
4. V. Mares, H. Schraube, Proceedings, The IRPA Regional Symposium on Radiation Protection in Neighbouring Countries of Central Europe, Prague, Czech Republic, September 1997, 543-547, (1998) http://www.iaea.org/inis/collection/NCLCollectionStore/_Public/30/031/30031466.pdf
5. V. Mares, G. Schraube, H. Schraube, Nucl. Instr. Meth. A **307**, 398–412 (1991)
6. V. Mares, A. Sannikov, H. Schraube, SATIF-3 Proceedings, Sendai, Japan, 237-248 (1998)
7. A.V. Alevra, M. Cosack, J.B. Hunt, D.J. Thomas, H. Schraube, Radiat. Prot. Dosim. **40**, 91-10 (1992)
8. D.J. Thomas, A.V. Alevra, J.B. Hunt, H. Schraube Radiat. Prot. Dosim. **54**, 25-31 (1994)
9. V. Mares et al., IEEE Trans. Nucl. Sc. **60**, 299-304 (2013)
10. M. Matzke, Private communication later integrated into the neutron metrology file IAEA1279 ZZ-NMF-90 available from NEA Databank (1987)
11. ICRP, International Commission on Radiological Protection, ICRP Publication 74. Pergamon (1997).
12. M. Pelliccioni, Radiat. Prot. Dosim. **88,** 279–297 (2000)
13. R. Nolte, M.S. Allie, P.J. Binns, F. Brooks, A. Buffler, V. Dangendorf, J.P.Meulders, F. Roos, H. Schuhmacher, B. Wiegel, Nucl. Instr. and Meth. A 476, 369-373 (2002)
14. V. Mares, A. V. Sannikov, and H. Schraube, Nucl. Instrum. Methods Phys. Res., Sect. A 476, 341‑346 (2002)
15. ISO/DIS 8529-1 2001, International Organization for Standardization, Geneva, Switzerland (2001)
16. J. W. Leake, T. Lowe, R.S. Mason, Nucl. Instr. and Meth. A 519 (2004) 636–646
17. M. Wielunski, R. Schutz, E. Fantuzzi, A. Pagnamenta, W. Wahl, J. Palfalvi P. Zombori, A. Andrasi, H. Stadtmann, and C. Schmitzer, Nucl. Instr. And Meth. A 517 (2004).240‑253

18. F. Bergmeier, M. Volnhals, M. Wielunski, and W. Rühm, Radiat. Prot. Dosim. 161 (2013) 126‑129
19. R. H. Olsher, T. D. McLean, A. L. Justus, R. T. Devine, and M. S. Gadd, Radiat. Prot. Dosim. 138, (2010), 199-204